Optics Letters

High-reflection Mo/Be/Si multilayers for EUV lithography

Nikolai I. Chkhalo,[1,*] Sergei A. Gusev,[1] Andrey N. Nechay,[1] Dmitry E. Pariev,[1] Vladimir N. Polkovnikov,[1] Nikolai N. Salashchenko,[1] Franz Schäfers,[2] Mewael G. Sertsu,[2] Andrey Sokolov,[3] Mikhail V. Svechnikov,[1] and Dmitry A. Tatarsky[1]

[1]Institute for Physics of Microstructures RAS, GSP-105, 603950 Nizhny Novgorod, Russia
[2]Department of Nanooptics and Technology, Helmholtz-Zentrum Berlin, Albert-Einstein-Straße 15, D-12489 Berlin, Germany
[3]Department Precision Gratings, Helmholtz-Zentrum Berlin, Albert-Einstein-Straße 15, D-12489 Berlin, Germany
*Corresponding author: chkhalo@ipm.sci-nnov.ru

Received 7 September 2017; revised 3 November 2017; accepted 3 November 2017; posted 7 November 2017 (Doc. ID 306455); published 5 December 2017

The effect of Be layers on the reflection coefficients of Mo/Be/Si multilayer mirrors in the extreme ultraviolet (EUV) region is reported. Samples were studied using laboratory and synchrotron based reflectometry, and high-resolution transmission electron microscopy. The samples under study have reflection coefficients above 71% at 13.5 nm and more than 72% at 12.9 nm in a near normal incidence mode. Calculations show that by optimizing the thickness of the Be layer it should be possible to increase the reflection coefficient by another 0.5–1%. These results are of considerable interest for EUV lithography.

OCIS codes: (340.7480) X-rays, soft x-rays, extreme ultraviolet (EUV); (340.7470) X-ray mirrors; (310.4165) Multilayer design; (310.1860) Deposition and fabrication; (220.3740) Lithography.

https://doi.org/10.1364/OL.42.005070

One of the key problems in the production of integrated circuits using extreme ultraviolet (EUV) lithography at a wavelength of 13.5 nm is insufficient lithographic performance. The output is directly proportional to the conversion coefficient of laser radiation energy into EUV of highly charged Sn ions, and to the Nth power ($N \approx 11$ is the number of mirrors in the lithographer's optical scheme [1]) of the reflection coefficient of Mo/Si multilayer mirrors (MLMs). The progress of recent years in increasing the EUV lithography productivity is associated with an increase in the conversion coefficient of the laser radiation energy into EUV and with the increase in the power of the laser system [2].

However, the power-law dependence of the efficiency on the reflection coefficient of the mirrors makes it extremely urgent to find ways to increase the reflection coefficient of the Mo/Si MLM. Moreover, even a slight increase in the reflection coefficient, for example, from 70 to 72%, will lead to an increase in the productivity of the 11-mirror (including the mask) lithographic system by 1.36 times, resulting in a large economic effect. Of course, to determine real performance, the spectral throughput of the optical system should be integrated with the source function. Nevertheless, optimizing the peak reflectivity values is of great interest. The main method of increasing reflection coefficients of Mo/Si mirrors is interface engineering, with the main task of improving the Mo-on-Si boundary. As a result, the maximum reflectivity of 70.15% at a wavelength of 13.5 nm and up to 71.0% at a wavelength of 12.7 nm was achieved through the minimization of the inter-diffusion processes in the interface-engineered Mo/B_4C/Si/B_4C and Mo/Si/C MLMs [3–5]. Subsequently, work on Mo/Si mirrors mainly concerned the physical aspects of interface formation [6–8] and increase in their resistance to heating and oxidation [3,9,10], and did not lead to an increase in the reflection coefficients.

In [11] (unpublished to date), when studying the influence of the interlayers of different materials on the reflection coefficients of the Mo/Be MLM at wavelengths of 0.154 and 11.3 nm, we first showed that the Si interlayers deposited on the Be layers lead to a significant sharpening of the Be-on-Mo boundary (in root-mean-square sense). Since Si is a highly absorbing material near 11.3 nm wavelength, it reduces the EUV reflectivity, but its impact on the other boundary shows an indirect sharpening. Figure 1 shows grazing incidence x-ray reflectivity (GIXR) curves for the Mo/Be and Mo/Be/Si MLM obtained with a laboratory diffractometer at a wavelength of 0.154 nm. In Table 1, the main characteristics of these two kinds of MLMs are given. Parameters were obtained from simultaneous fitting of reflectivity curves at $\lambda = 0.154$ nm and $\lambda = 11.3$ nm. The two structures have the same number of periods and the same average period. The Mo/Be MLM has a slightly bigger thickness drift (~0.014% per period) than Mo/Be/Si (~0.01% per period). Thicknesses of Mo are very close to each other; although Table 1 states that the difference between Mo thicknesses is 0.1 nm, it cannot be established with such accuracy after reflectometric fitting. In reality, in-depth resolution of the method in its current form is about 0.1–0.2 nm.

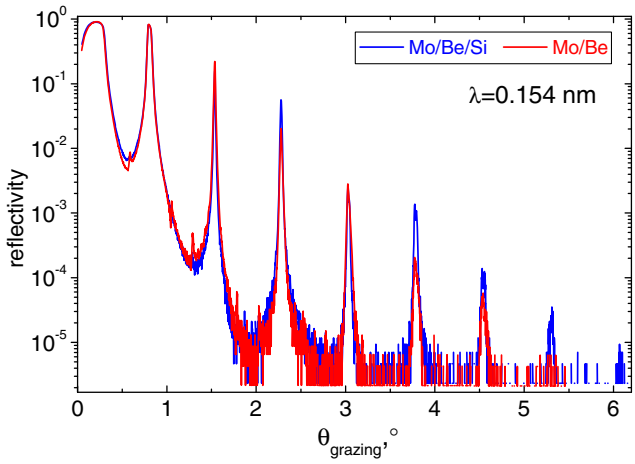

Fig. 1. Measured GIXR curves of Mo/Be and Mo/Be/Si MLMs, intended for 11.3 nm wavelength. Reconstructed parameters of structures are given in Table 1.

The major difference between structures is the effective width of Be-on-Mo boundary. Introduction of a thin Si interlayer into the MLM has diminished its value from 0.36 to 0.27 nm. When the interlayer is introduced, it influences both boundaries, because the growth conditions for subsequent layers become different. In work [12], the introduction of a 1 nm Si interlayer between 3.85 nm Al and 4.05 nm Be films led to strong smoothing of both boundaries, from 1.3 to 0.6 nm via amorphization. Here it can be a similar effect, but in weaker form. Definitely, this improvement is the main reason for the visibility of the high-order Bragg peaks of the Mo/Be/Si MLM in Fig. 1. In contrast to this, the high orders of the Mo/Be MLM decay faster.

The results of the x-ray reconstruction are qualitatively well confirmed by the data of high-resolution transmission electron microscopy (TEM) of the MLM's cross sections. The cross sections were prepared at a double beam Quanta 3D FEG facility using focusing ion beam technology, described for example in [13]. TEM measurements were done with a high-resolution transmission electron microscope LIBRA 200 MC. In Fig. 2, a TEM image of the fragment of the similar Mo/Be/Si MLM's cross section (a) and the cross-sectional profile averaged over the 100 lines marked in the TEM image (b) is shown. The minimum on the profile corresponds to the Mo layers; the maximum corresponds to Be layers, and in between them attributes to Si layers. Parameters of the sample shown in Fig. 2 are close to that of the sample shown in Table 1. According to

Table 1. Main Characteristics of the Mo/Be and Mo/Be/Si Samples, Tested for 11.3 nm Wavelength[a]

MLM	N	$\langle d\rangle$, nm	$\langle h(M)\rangle$, nm	Interface Width, nm
Mo/Be	110	5.85	h(Be) = 3.61	Mo – on – Be = 0.73
			h(Mo) = 2.24	Be – on – Mo = 0.36
Mo/Be/Si	110	5.85	h(Si) = 0.43	Mo – on – Si = 0.74
			h(Be) = 3.09	Si – on – Be = 0.15
			h(Mo) = 2.33	Be – on – Mo = 0.27

[a]N is the number of periods, $\langle d\rangle$—average period, $\langle h(M)\rangle$—average film thicknesses.

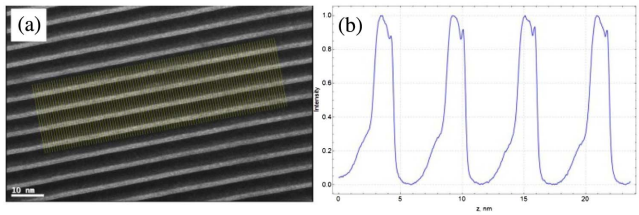

Fig. 2. TEM image of (a) a fragment of the cross section of a Mo/Be/Si MLM and (b) the cross-sectional profile averaged over 100 lines marked in the TEM image.

this cross section, the Mo thickness can be estimated to be 2.3 nm, Be—2 nm; the transition region between Mo and Be, including the Si layers is 1.5 nm. The smallest transition region is observed at the Be-on-Mo boundary, which is 0.2–0.3 nm. Apparently, as in classical Mo/Si mirrors, the Mo-on-Si boundary is a molybdenum silicide [3–5,14,15]. The width of the Si-on-Be boundary is not well established by reflectometry due to its comparatively low optical contrast, so the corresponding value in Table 1 is not precise.

Thus, we have clear evidence of sharpening the Be-on-Mo boundary in the presence of a Si interlayer on another boundary. Consequently, we can expect the same effect for the Mo/Be/Si structure with full-grown layers of Be and Si. Below we describe the efficiency of the ternary structure for 13.5 nm.

According to Henke tables [16], Be has the smallest absorption in the vicinity of 13.5 nm, even smaller than Si. This material looks optically favorable for being used as the third layer in the Mo/Si MLM in order to increase reflection coefficients in the EUV region. For example, in [17], the authors tried to optimize three- and four-component MLMs with different orders of Mo, Be, and Si in the period. Calculations show that an ideal MLM with optimized thicknesses of Mo, Si, and Be films has a 1% higher reflection coefficient at 13.5 nm and at normal incidence, as compared with the corresponding ideal Mo/Si MLM. In practice, given the quality of the interfaces, one can expect an even more powerful effect of Mo/Be/Si over conventional Mo/Si MLMs.

We also optimized four kinds of MLMs for the best peak reflectivity; results are given in Table 2. IMD software [18] with optical constants [16] was used for the optimization. The structures listed in Table 2 were supposed to be ideal.

It can be seen from the table that ideal structures have a comparable reflectivity bandwidth, while the Mo/Be/Si structure can provide higher reflectivity. Real structures have blurred boundaries, so real $\Delta\lambda_{1/2}$ values will be lower.

To investigate the effect of Be layers on reflectance in EUV range, a series of the Mo/Be/Si MLM were fabricated by direct

Table 2. Comparative Table of Ideal Structures, Optimized for Maximal Reflectivity[a]

Structure, nm	N	$\Delta\lambda_{1/2}$, nm	R, %
Mo(2.54)/Be(1.41)/Si(2.96)	110	0.556	75.1
Mo(2.67)/Si(4.23)	110	0.573	74.0
Mo(2.34)/B_4C(0.3)/Si(3.96)/B_4C(0.3)	110	0.567	72.9
Mo(2.48)/Si(4.12)/C(0.3)	110	0.570	73.8

[a]The boundaries are sharp ($\sigma = 0$). The thicknesses of B_4C and C were fixed during optimization. $\Delta\lambda_{1/2}$ is a spectral bandwidth at half-maximum.

current magnetron sputtering. For more information on the sputtering regimes, see [12]. The study of the structural parameters of the MLM, such as the period and its systematic change in depth, thickness, and density of the films, and the type of transition regions, was carried out by the method of simultaneous fitting of the angular dependencies of x-ray reflection coefficients at wavelengths of 0.154 nm and in the vicinity of 13.5 nm. The specific wavelengths for each sample are given in the tables below. To do this, for the first time, to the best of our knowledge, an extended model for reconstructing the internal structure of the MLM from x-ray reflection data was used [19].

Measurements at a wavelength of 0.154 nm were made using a PANalytical X'Pert PRO diffractometer equipped with a four-crystal Ge (220) monochromator. Preliminary measurements at a wavelength of 13.5 nm were carried out on a laboratory reflectometer with a Si x-ray tube as a radiation source. The monochromatization of the radiation was carried out using a grazing incidence grating monochromator that provided the spectral width of the probing beam $\delta\lambda = 0.03$ nm ($\lambda/\delta\lambda \approx 380$). The reflectometer is described in detail in [20]. Precise measurements of the reflection coefficients in the EUV region, the values of which are given in this Letter, were carried out at the at-wavelength metrology facility with an 11-axis reflectometer end station on the optics beamline of the BESSY-II synchrotron radiation source [21,22]. The accuracies of measurements were ±0.02% to wavelength scale, 0.02° to angular scale, and spectral impurity of incident radiation smaller than 0.01%. The incident beam size in the experiment was about 0.6 mm × 0.25 mm ($v * h$). The detector active area of 4 × mm × 4 mm was enough to accept specular and most of the scattered part of reflected beam.

The main characteristics of the samples under study are given in Table 3. For the most successful sample D387 in Fig. 3 are presented the measured (curves with symbols) and fitted (solid lines) angular dependencies of the reflection coefficients taken in different wavelengths: 0.154, 5.904, 9.534, 12.93, 13.49, and 13.78 nm. Figure 3 illustrates the following. First, the extended model of MLM parameter reconstruction used in this Letter showed its effectiveness; the simulated and measured angular dependencies of the reflection coefficients perfectly coincided in a wide range of wavelengths. Secondly, as expected, various interfaces were described in the best way by different functions, namely, the Mo-on-Si

Table 3. Main Characteristics of the Samples under Study[a]

Sample	N	$\langle d \rangle$, m	$\langle h(M) \rangle$, nm	Interface Width, nm
D385	110	6.949	h(Si) = 2.75	Mo – on – Si = 0.54
			h(Be) = 2.06	Si – on – Be = 0.73
			h(Mo) = 2.14	Be – on – Mo = 0.23
D386	110	6.971	h(Si) = 2.55	Mo – on – Si = 0.60
			h(Be) = 2.27	Si – on – Be = 0.63
			h(Mo) = 2.15	Be – on – Mo = 0.22
D387	110	7.060	h(Si) = 2.68	Mo – on – Si = 0.57
			h(Be) = 2.03	Si – on – Be = 0.84
			h(Mo) = 2.35	Be – on – Mo = 0.22
D388	110	6.918	h(Si) = 2.30	Mo – on – Si = 0.42
			h(Be) = 2.19	Si – on – Be = 0.74
			h(Mo) = 2.43	Be – on – Mo = 0.22

[a]All the presented samples have the same structure $Si_{substrate}$/(Mo/Be/Si) × N/air, where N is the number of periods, $\langle d \rangle$—average period thicknesses, $\langle h(M) \rangle$—average film thicknesses.

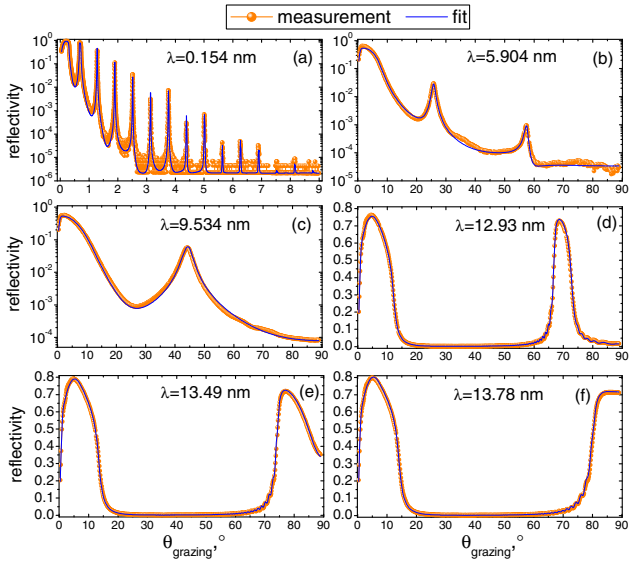

Fig. 3. Angular dependencies of the reflection coefficient of sample D387, taken and fitted at wavelengths (a) 0.154, (b) 5.904, (c) 9.534, (d) 12.93, (e) 13.49, and (f) 13.78 nm.

boundary was described by "exp" function, Si-on-Be—"step" and Be-on-Mo—"erf" function. Moreover, these functions turned out to be the same for all the studied structures, with the only difference being that in two cases the function of the first boundary with "erf" function is replaced by "linear" and "exp," However, taking into account the small value of the parameter $\sigma \approx 0.2$ nm, this difference is of no fundamental importance.

Table 4 shows the reflective characteristics of the series of four mirrors, described in Table 3, measured at BESSY-II.

Table 4. Reflective Characteristics of Mo/Be/Si MLMs Measured in the EUV Range at BESSY-II in s-Polarization[a]

MLM	Film Thickness, nm	Measurement Type	λ, nm	θ, °	R, %
D385	Mo(2.14)/ Be(2.059)/ Si(2.75)	spectral $\Delta\lambda_{1/2} = 0.477$ nm	13.63	88.0	71.11
		angular	13.53	81.9	71.12
		angular	13.49	80.9	71.15
		angular	13.04	72.2	71.97
D386	Mo(2.15)/ Be(2.271)/ Si(2.55)	spectral $\Delta\lambda_{1/2} = 0.485$ nm	13.66	88.0	70.82
		angular	13.53	81.0	71.1
D387	Mo(2.35)/ Be(2.03)/ Si(2.68)	spectral $\Delta\lambda_{1/2} = 0.515$ nm	13.8	88.0	71.3
		angular	13.78	86.1	71.42
		angular	13.49	77.1	71.89
		angular	13.20	72.3	72.32
		angular	12.92	68.7	72.83
D388	Mo(2.43)/ Be(2.19)/ Si(2.30)	spectral $\Delta\lambda_{1/2} = 0.524$ nm	13.87	88.0	70.20
		angular	13.49	76.0	71.40

[a]$\Delta\lambda_{1/2}$ is a spectral bandwidth at half-maximum.

In the first column, there is the mirror identifier; in the second column, there is the MLM composition with layer thicknesses; in the third column, there is the measurement type and the spectral width of the reflection curve measured at the angle of 88°; in the fourth column, there is the wavelength; in the fifth column, there is the Bragg grazing angle; in the sixth column, there is the maximum of the reflection coefficient. As can be seen from the table, all the samples under study in the vicinity of the wavelength of 13.5 nm have reflection coefficients exceeding 71%. In particular, at a wavelength of 12.92 nm, the reflection coefficient was 72.83% (*s*-polarization, 68.7°) and at a wavelength of 13.49 nm it reaches 71.89% (*s*-polarization, 77.1°). At 2° from normal at a wavelength of 13.8 nm, it was 71.34%. All these values are records and exceed by more than 1% the reflection coefficients of the Mo/Si mirrors with C and B_4C antidiffusion layers [3,4].

It should be noted that none of the samples studied had the optimal layer thicknesses required to achieve the maximum reflection coefficient at 13.5 nm at normal incidence. In all the samples studied, the thickness of Be exceeded by several angstroms the optimum, and the thickness of molybdenum, in contrast with the exception of sample D388, was smaller. The sample D387, whose layer thickness ratio was closest to the optimal values, showed the highest reflection coefficients. Therefore, we expect that in the next series of experiments that we will be able to increase the reflection coefficient of Mo/Be/Si mirrors by 0.5–1% by optimizing the film thicknesses.

In the described experiments, Be was deposited only onto one boundary, while the Mo-on-Si boundary, which is problematic in the classical Mo/Si MLM, was not subject to the application of the interface engineering. The improvement of the Mo-on-Si boundary can also lead to an additional increase in the reflection coefficients of the Mo/Be/Si MLM.

In conclusion, the Letter showed that with the help of Be layers it was possible to increase the reflection coefficients of the Mo/Si MLM in the EUV range by 1–2%. Moreover, by optimizing film thicknesses in the MLM and using interface engineering on the Mo-on-Si boundary, an even higher increment of the reflection coefficient can be expected. Apparently, the most promising structure seems to be $Mo/Be/Si/B_4C$. We believe that this result is of considerable interest for EUV lithography, since it can significantly increase the productivity of the lithographic process if a Mo/Be/Si MLM is used instead of classical Mo/Si mirrors. Nevertheless, the new kind of structure should be optimized not only for peak reflectance but from the point of integral performance, and its thermal, oxidative, and mechanical properties should be exhaustively investigated.

Funding. Russian Foundation for Basic Research (RFBR) (15-02-07753, 17-52-150006); Russian Science Foundation (RSF) (16-42-01034); Deutsche Forschungsgemeinschaft (DFG) (SO 1497/1-1).

Acknowledgment. The authors thank the staff of the company Sernia (Moscow, Russia), who prepared the Mo/Be/Si MLM slice for electron microscope studies and HZB for the allocation of synchrotron radiation beam time.

REFERENCES

1. A. Pirati, J. van Schoot, K. Troost, R. van Ballegoij, P. Krabbendam, J. Stoeldraijer, E. Loopstra, J. Benschop, J. Finders, H. Meiling, E. van Setten, N. Mika, J. Dredonkx, U. Stamm, B. Kneer, B. Thuering, W. Kaiser, T. Heil, and S. Migura, Proc. SPIE **10143**, 101430G (2017).
2. A. A. Schafgans, D. J. Brown, I. V. Fomenkov, Y. Tao, M. Purvis, S. I. Rokitski, G. O. Vaschenko, R. J. Rafac, and D. C. Brandt, Proc. SPIE **10143**, 101431I (2017).
3. S. Bajt, J. Alameda, T. Barbee, W. M. Clift, J. Folta, A. Kaufmann, and E. A. Spiller, Opt. Eng. **41**, 1797 (2002).
4. S. Braun, H. Mai, M. Moss, R. Scholz, and A. Leson, Jpn. J. Appl. Phys. **41**, 4074 (2002).
5. A. E. Yakshin, R. W. E. van de Kruijs, I. Nedelcu, E. Zoethout, E. Louis, F. Bijkerk, H. Enkisch, and S. Müllender, Proc. SPIE **6517**, 65170I (2007).
6. I. Nedelcu, R. W. E. van der Kruijs, A. E. Yakshin, and F. Bijkerk, Phys. Rev. B **76**, 245404 (2007).
7. A. Haase, V. Soltwisch, F. Scholze, and S. Braun, Proc. SPIE **9628**, 962804 (2015).
8. J. Zhao, H. He, H. Wang, K. Yi, B. Wang, and Y. Cui, Chin. Opt. Lett. **14**, 083401 (2016).
9. S. L. Nyabero, A. R. W. E. van de Kruijs, A. A. E. Yakshin, A. E. Zoethout, and A. F. Bijkerk, J. Appl. Phys. **112**, 054317 (2012).
10. T. Feigl, H. Lauth, S. Yulin, and N. Kaiser, Microelectron. Eng. **57–58**, 3 (2001).
11. N. I. Chkhalo, A. N. Nechay, D. E. Pariev, V. N. Polkovnikov, N. N. Salashchenko, F. Schäfers, A. Sokolov, M. V. Svechnikov, Yu. A. Vainer, M. V. Zorina, and S. Yu. Zuev, *Physics of X-Ray and Neutron Multilayer Structures Workshop*, University of Twente, The Netherlands, November 10th–11th, 2016.
12. N. I. Chkhalo, D. E. Pariev, V. N. Polkovnikov, N. N. Salashchenko, R. A. Shaposhnikov, I. L. Stroulea, M. V. Svechnikov, Yu. A. Vainer, and S. Yu. Zuev, Thin Solid Films **631**, 106 (2017).
13. R. M. Langford and A. K. Petford-Long, J. Vac. Sci. Technol. A **19**, 2186 (2001).
14. S. Yulin, T. Feigl, T. Kuhlmann, N. Kaiser, A. I. Fedorenko, V. V. Kondratenko, O. V. Poltseva, V. A. Sevryukova, A. Yu. Zolotaryov, and E. N. Zubarev, J. Appl. Phys. **92**, 1216 (2002).
15. A. E. Yakshin, E. Louis, P. C. Görts, E. L. G. Maas, and F. Bijkerk, Physica B **283**, 143 (2000).
16. B. L. Henke, E. M. Gullikson, and J. C. Davis, At. Data Nucl. Data Tables **54**, 181 (1993).
17. S. M. Al-Marzoug and R. J. Hodgson, Appl. Opt. **47**, 2155 (2008).
18. D. L. Windt, Comput. Phys. **12**, 360 (1998).
19. M. Svechnikov, D. Pariev, A. Nechay, N. Salashchenko, N. Chkhalo, Y. Vainer, and D. Gaman, J. Appl. Cryst. **50**, 1428 (2017).
20. M. S. Bibishkin, D. P. Chekhonadskih, N. I. Chkhalo, E. B. Klyuenkov, A. E. Pestov, N. N. Salashchenko, L. A. Shmaenok, I. G. Zabrodin, and S. Yu. Zuev, Proc. SPIE **5401**, 8 (2004).
21. F. Schäfers, P. Bischoff, F. Eggenstein, A. Erko, A. Gaupp, S. Künstner, M. Mast, J.-S. Schmidt, F. Senf, F. Siewert, A. Sokolov, and Th. Zeschke, J. Synchr. Rad. **23**, 67 (2016).
22. A. Sokolov, P. Bischoff, F. Eggenstein, A. Erko, A. Gaupp, S. Künstner, M. Mast, J.-S. Schmidt, F. Senf, F. Siewert, Th. Zeschke, and F. Schäfers, Rev. Sci. Instrum. **87**, 052005 (2016).